A simple method for sizing and estimating the performance of PV systems in trolleybus grids

Diab, Ibrahim; Saffirio, Alice ; Chandra-Mouli, Gautham Ram; Bauer, Pavol

DOI
10.1016/j.jclepro.2022.135623

Publication date
2023

Document Version
Final published version

Published in
Journal of Cleaner Production

Journal of Cleaner Production 384 (2023) 135623

Contents lists available at ScienceDirect

Journal of Cleaner Production

journal homepage: www.elsevier.com/locate/jclepro

A simple method for sizing and estimating the performance of PV systems in trolleybus grids☆

Ibrahim Diab *, Alice Saffirio, Gautham Ram Chandra-Mouli, Pavol Bauer

Technische Universiteit Delft (TU Delft), Faculty of Electrical Engineering, Mathematics, and Computer Science, Electrical Sustainable Energy Department, Mekelweg 4, 2628 CD Delft, The Netherlands

ARTICLE INFO

Handling Editor: Panos Seferlis

Keywords:
DC systems
Electrical transportation
Public transport
PV systems
Regenerative braking
Trolleybus

ABSTRACT

Solar PV systems have so far been the source of choice for the sustainable supply of urban electric transport networks—like trams and trolleybus grids. However, no consensus exists yet on the placement or sizing of PV systems at the traction substations, and no method is available for easy estimation of the PV system utilization performance. The latter is crucial for understanding the need for storage, grid exchange, or even power curtailment, and has therefore a direct impact on the technical and financial feasibility of the project.

This paper looks at 11 Key Performance Indicators (KPI) that are available to trolleybus operators, in two PV case studies on Arnhem (NL) and Gdynia (PL), using verified and validated bus, grid, and PV models. Through one KPI, namely the here-defined Energy Traffic KPI, a strong trend (R^2=0.93) is described that can now allow stakeholders a quick estimation of the PV potential using a simple third-degree polynomial instead of resorting to the complex grid, bus, and PV modelling. A simple placement and sizing method is also presented derived from this KPI, in a way as to increase the technical and economical feasibility of an installed PV system. Despite all efforts, stakeholders are still warned of an intrinsic, upper-performance plateau that exists in transport grids, at around 38% direct PV utilization, caused by the unavoidable mismatch between PV generation and vehicle timetables and schedules. Stakeholders are urged to implement more smart grid loads as a base load to increase the feasibility of their investments in renewables, and to transform the transportation systems thereby to multi-functional grids that can assist the main city grid.

1. Introduction

While the electrification of urban transportation is already a mature and efficient method of sustainable urban transport (Bartłomiejczyk and Połom, 2017), the solution is only meaningful if the supply power comes from sustainable sources. So far, the global transport sector still relies heavily on fossil fuels and accounts for about 24% of total GHG emissions (IEA, 2020; Wang et al., 2007). In Europe, this number stands at 40% (Bartłomiejczyk and Kołacz, 2020).

PV systems are an attractive solution for the sustainable electrification of transport networks as they are DC systems like these networks, scalable, and easy to install in an urban environment. So far, PV systems are the most promising and also most implemented source for this type of application (Diab et al., 2022e; Bartłomiejczyk, 2018b; Wazifehdust et al., 2019; Salih et al., 2018; Diab et al., 2022c; Liu et al., 2021; Zhu et al., 2019; Zahedmanesh et al., 2021; Diab et al., 2022b,a). However, there is still no consensus on methods of PV sizing or placement, and no readily accessible ways for grid operators to estimate the success and performance of these systems except by outsourcing detailed, complex, and costly modelling tools (Diab et al., 2022e).

1.1. The trolleybus grid with PV

The trolleybus is an electric bus that is supplied by overhead lines (catenary), similar to the way a tram operates. From the Low Voltage AC (LVAC), a substation (step-down transformer and a rectifier) supplies the buses on its sections via feeder cables, at 650–750Vdc, depending on the city, as shown in Fig. 1 (Diab et al., 2022e,d; Hamacek et al., 2014; Bartłomiejczyk and Połom, 2015a; Bartłomiejczyk, 2018a). The minimum bus voltage for operation is 400 V, consequently, the trolleybus lines are divided into isolated sections to limit the resistive voltage drops in the catenary and transmission losses, and for reasons such as fault protection. The sections are a few hundred meters in length, up to 1 or 2 km, depending on the trolleygrid city.

☆ This research was funded by Trolley2.0 under Electric Mobility Europe.
* Corresponding author.
E-mail address: i.diab@tudelft.nl (I. Diab).

https://doi.org/10.1016/j.jclepro.2022.135623
Received 19 October 2022; Received in revised form 28 November 2022; Accepted 12 December 2022
Available online 14 December 2022

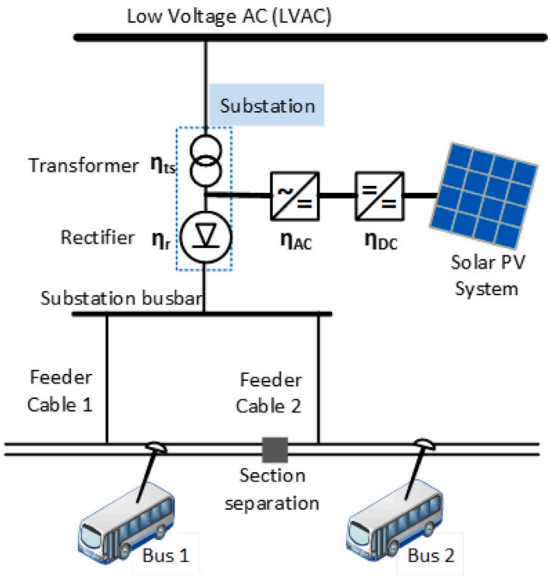

Fig. 1. The PV-powered trolleygrid and its components. Here, the PV is connected to the AC side to avoid installing costly storage systems for the excess PV energy.

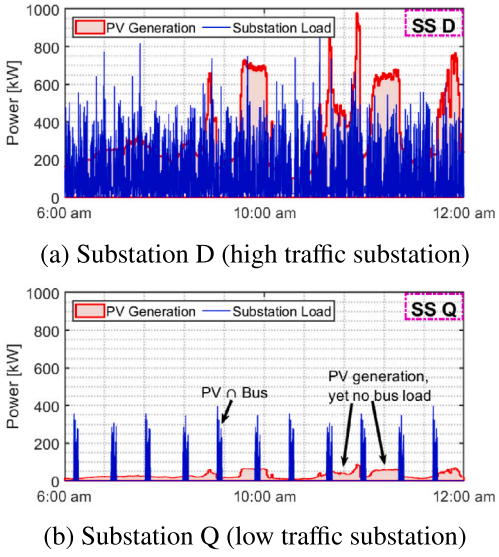

(a) Substation D (high traffic substation)

(b) Substation Q (low traffic substation)

Fig. 2. Mismatch in PV generation and the bus load for two substations in the city of Arnhem, the Netherlands.
Source: Simulation results from Diab et al. (2022e).

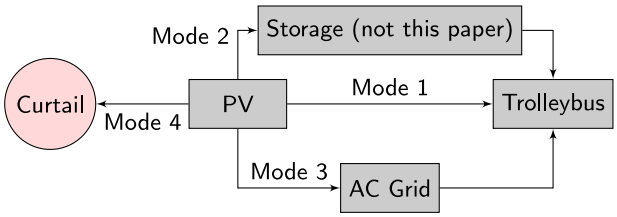

Fig. 3. Generated PV energy can be used directly by the trolleybus (mode 1, most desirable), stored for later trolleygrid use (mode 2, not in this paper), exchanged with the AC Grid (mode 3, net metering), or curtailed (mode 4, wasted).

Trolleybuses consume about 70 kW of traction power during regular driving and can reach power peaks higher than 300 kW while accelerating. When a trolleybus brakes, the available regenerative braking power can be as high as 200 kW. In the absence of on-board storage, this power can be shared with buses on the same section, on a connected section under the same substation (Bus1 and Bus2 in Fig. 1), or wasted in on-board braking resistors (Tomar et al., 2018; Zhang et al., 2015, 2017). The braking energy cannot be sent back to the LVAC grid because of the rectifiers at the substation. This would also apply to the PV excess energy if the PV is connected on the DC side of the trolleygrid, for example at the substation bus bar or directly on the section (see Fig. 1 for nomenclature).

Unfortunately, the trolleybuses run on a schedule with some time intervals between vehicles, like any public transportation system. This results in low-traffic substations experiencing long periods of zero bus demand during which the PV system is generating unused power. This is referred to as low direct PV utilization and is presented in Fig. 2(b) for substation Q of the city of Arnhem, the Netherlands, where the blue line shows the substation load demand, and the red line shows the generation of a connected PV system sized for energy neutrality.

On the other hand, the busier substation D of Fig. 2(a) seems to promise a high direct PV utilization. A large mismatch also happens during the night as the PV system does not generate power at all, while the buses would still be operating. This creates the main challenge for PV integration when hoping for energy-neutral sizing, by necessitating expensive storage systems and/or an exchange with the LVAC grid (if net-metering is allowed). An even less desirable solution is to curtail the generated PV energy (waste), which could render the PV system integration economically unfeasible (Diab et al., 2022e; Bartłomiejczyk and Połom, 2017). These possible PV power flows, summarized in Fig. 3, need to be estimated and understood early in advance by the stakeholders to gauge the economic and technical feasibility of a PV project.

Unfortunately, no such tool exists yet without resorting to expensive studies that detail the grid and the PV in great detail. The research in this paper hopes to offer a solution to bridge that gap.

1.2. The trolleybus grid with PV in literature

The sizing and placement of PV systems in trolleygrids and the degree of independence they can offer from the LVAC grid is an understudied field. This lack of research leaves trolley cities unable to estimate -or worse, unaware of-their PV potential. For example, as seen in the literature and in this paper, the direct utilization of the generated PV system power by trolleybus(es) can vary significantly from substation to substation within the same city, from around 10% to 80% (Bartłomiejczyk, 2018b; Wazifehdust et al., 2019; Diab et al., 2022e).

This creates the urgent need for an estimation method for the PV performance in trolleygrids, to avoid the installation of economically unfeasible PV systems at low-potential substations and/or at non-optimal system sizes. So far, the studies in the literature have been mostly statistical, limited to one PV system size, and did not go in-depth into analysing the causes of these differences, nor offer simple ways to predict the PV performance at different substations (Bartłomiejczyk, 2018b; Wazifehdust et al., 2019; Salih et al., 2018; Liu et al., 2021; Zhu et al., 2019; Zahedmanesh et al., 2021; Kratz et al., 2019; Salih et al., 2019). This paper presents a method for this purpose.

1.3. Paper contributions

This paper offers the following 4 contributions:

1. A thorough study and assessment framework for the PV system direct utilization and load coverage at a single trolleygrid substation as a function of a number of readily-available grid parameters to the transport grid stakeholders using detailed and validated bus, grid, and PV models and two trolleybus countries as case studies (The Netherlands and Poland)

2. A simple, empirically-identified, three-variable function that allows stakeholders to quickly estimate and assess the potential and performance of a PV system of any size connected to a single trolley substation, instead of requiring a complex grid, PV, and bus modelling
3. The identification of a saturation plateau in the PV system performance at a single substation that challenges what has been previously reported in the literature that larger substations would always report a better PV utilization
4. A proposed methodology for the sizing of a decentralized PV system shared by a group of neighbouring substations for increasing the system performance, based on a simple, empirically-identified, three-variable function instead of the complex grid, PV, and bus modelling

1.4. Paper structure

The paper begins with an explanation of PV integration in trolleybus grids. Section 2 details the methodology and models used. Section 3 presents the results of the KPI study (Contributions 1 and 2). Section 4 explains the formulated third-degree polynomial for the PV system performance estimation (Contribution 2). This is expanded in Section 5 into an advised methodology for the sizing of these systems and their placement (Contribution 3). Finally, Section 6 offers some conclusions and future work recommendations.

2. Methodology

To study the mismatch between the trolleygrid load and the PV generation, the following three subsections present first the PV system placement, then the modelling methodology for the load (the individual buses and then the substations), and finally the PV output power modelling. In Section 2.4, some performance indicators are defined to assess the utilization of the PV system. Section 2.5 introduces the two case study cities used in this paper.

2.1. PV system placement

For this paper, the PV and storage are installed on the AC side (Fig. 1), which admittedly reduces the efficiency of the connection, since the generated solar energy has to be converted from DC to AC and then back to DC to supply the buses. However, while alternatively installing the PV on the DC side would reduce the system losses by using fewer power conversion steps, this configuration would not allow the PV to send its excess energy back to the main AC grid (substation diode rectifiers). Even if storage is installed, considerable curtailment of the PV power is expected, as the required seasonal storage would be unrealistically large (Salih et al., 2019; Wazifehdust et al., 2019). Moreover, placing the PV system on the DC side could introduce strong voltage fluctuations on the section due to the intermittent PV power generation and the difficulty of gauging an output set-point. This is because the short-term variability of the PV output can present power fluctuations of 45%–90% of the rated power of the system, and would indeed require more sophisticated converters for the trolleygrid stability (Brinkel et al., 2020; Bartłomiejczyk, 2018b; Kratz et al., 2018).

Another solution is to replace the unidirectional substations with reversible or bidirectional substations equipped with inverters that allow exchange from the DC to the AC side (Warin et al., 2011; Bartłomiejczyk and Połom, 2015b) from both the PV and the braking buses. However, this requires an overhaul of the trolleygrid infrastructure and is out of the scope of this paper.

For these reasons, the PV system is placed in this paper on the AC side for the PV integration in the trolleybus grid.

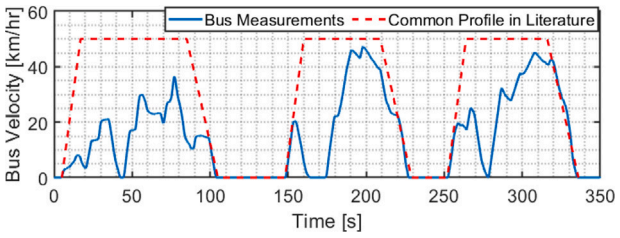

Fig. 4. The more realistic bus velocity measurements used in this paper compared to the trapezoidal velocity profile commonly found in literature.

2.2. Trolleybus and trolleygrid models

The trolleybus and trolleygrid modelling is performed by verified and peer-reviewed models that are explained in detail by the authors of this paper in Diab et al. (2022d,e).

In short, the simulation model begins with the creation of bus power demands and positions from a database of measured bus velocity and power cycles, timetables, and traffic light probability data. The parameters are created for a whole year with a 1-second time step, as the bus acceleration is at the order of seconds, and in accordance with other adopted time steps in literature (Paternost et al., 2022; Barbone et al., 2022; Chymera et al., 2010). These measurements help build a more realistic bus velocity and power cycles than that commonly found in the literature that ignores the effect of the city traffic and the traffic stoplights (Fig. 4).

The bus powers are given by Eq. (1). While in traction mode, the bus power, P_{bus}, is the traction power, P_{tr}, and the auxiliaries demand of the HVAC (Heating, Ventilation, and Air Conditioning) load, P_{HVAC}, and other base loads, P_{base}, such as the bus lighting, information screens, the door opening and closing motors, the control systems, etc. During braking, the bus power is the auxiliaries and base powers plus the net exchanged with the other buses P_{net}, and the excess energy, P_{BR}, that is wasted in the onboard braking resistors. The modelling of the HVAC is important to understand and model in detail as it can account for half of the bus load demand in winter in cold environments, and is the first recipient of the bus braking energy, which would otherwise go to feeding other buses on the section, changing thereby the power flow in the grid (Diab et al., 2022d; Tomar et al., 2018; Bartłomiejczyk and Kołacz, 2020).

$$P_{\text{bus}} = \begin{cases} P_{\text{tr}} + P_{\text{HVAC}} + P_{\text{base}}, & \text{traction} \quad j = 1..N_{\text{bus}} \\ P_{\text{net}} + P_{\text{HVAC}} + P_{\text{base}} + P_{\text{BR}}, & \text{braking} \end{cases} \tag{1}$$

$$I_{\text{n}} = \begin{cases} P_{\text{n}}/V_{\text{SN}} & k = 1, \quad \& \quad n \neq \text{SN} \\ P_{\text{n}}/V_{\text{n}} & k \neq 1, \quad \& \quad n \neq \text{SN} \\ -\sum_{n \neq \text{SN}} I_{\text{n}} & n = \text{SN} \end{cases} \tag{2}$$

$$R_{n,n-1} = \rho \cdot |x_n - x_{n-1}| \tag{3}$$

$$V_{\text{c}} = \begin{cases} V_{\text{SN}} - R_{\text{f}} \cdot I_{\text{SN}} & i_{\text{SN}} > 0 \\ V_{\text{SN}} + V_{\text{ds}} & i_{\text{SN}} = 0 \end{cases} \tag{4}$$

$$P_{\text{load}} = V_{\text{SN}} \cdot I_{\text{SN}} \tag{5}$$

The grid model is based on the backward-forward sweep method and is used to find the value of trolleygrid parameters such as the substation load demand, P_{load}, or the minimum line voltage on a trolleygrid section. The substation is modelled as a voltage-source slack node (SN), with a fixed nominal voltage, V_{SN}, at the rectifier output. For the first iteration step, k, the current at each node, I_n, is the power of that node, P_n, divided by V_{SN}, as an initial guess (Eq. (2)). At later iterations, the node voltage, V_n, from the previous step is used. The total impedance between two nodes n and $n-1$, $R_{n,n-1}$, is obtained from the equivalent impedance model (Eq. (3)) considering the specific impedance, ρ, and

the length, x, of the supply and return lines, and the effect of the parallel connections between the overhead lines. Typically this detailed analysis is ignored in literature (Iannuzzi et al., 2012; Finlayson et al., 2006). The voltage at the point of connection of the substation to the section, V_c, is given by Eq. (4), where R_f is the resistance of the feeder cable, I_{SN} is the substation current, and V_{ds} is the voltage blocked by the substation rectifiers in case of over-voltages on the section from regenerative braking. Feeder cables are also often ignored (except in works like (Sindi et al., 2018; Ku and Liu, 2002; Arboleya et al., 2018)). The slack node is then set to deliver the sum of all the node currents, and from that value, the substation load demand, P_{load}, is obtained (Eq. (5)). A convergence tolerance for all the node currents of 0.2 A is defined in this paper. For the first case study city in this paper, the Dutch city of Arnhem, this model has been verified against the grid's measured yearly energy demand to an error of 3% (Diab et al., 2022d).

For the other case study, the Polish city of Gdynia, not all the data related to the substation nominal voltage, the feeder cables, and the location of the feed-in points is available to the authors. Therefore, for Gdynia, the substation power demand is obtained as the sum of the simulated bus demands, increased by the measured transmission loss for each substation as reported in the measurements of the Gdynia trolleygrid in Bartłomiejczyk et al. (2016).

2.3. PV power output model

The PV model is a per-second simulation of the energy output of the solar panels. The model takes into accounts parameters such as solar altitude (a_S), solar azimuth (A_S), global horizontal irradiance (GHI), diffuse horizontal irradiance (DHI), ambient temperature, ground temperature, wind speed, etc. These values are obtained from Meteonorm (KNMI, 2019). The shading from clouds is considered. However, enough distance is assumed between panels to allow for panel-on-panel shading to be neglected.

The optimal azimuth angle and the tilt angle of the PV module are identified through an iteration, in which the yearly irradiance per square meter on the module is calculated for each possible combination of azimuth and tilt. At these positions, the global irradiance, G_M, on the model is:

$$G_M = G_{M,dir} + G_{M,diff} + G_{M,refl} \tag{6}$$

Where the terms on the right-hand side are the direct, diffuse, and reflected irradiance on the tilted module, respectively. The detailed equations for these terms are described in Smets et al. (2016). The PV module efficiency is a function of the module's temperature. This temperature is estimated as a function of meteorological parameters using a Fluid Dynamic model. The model is based on the energy balance between the PV module and the external surroundings, accounting for convection, conduction, and radiation heat transfers. The module's temperature, T_M, can be described as:

$$T_M = \frac{(1-R)(1-\eta)G_M + h_c T_a + h_{r,sky} T_{sky} + h_{r,gr} T_{gr}}{h_c + h_{r,sky} + h_{r,gr}} \tag{7}$$

Where R is the module reflectivity, η is the module's efficiency, h_c is the overall convective heat transfer coefficient (considering both top and back of the module), and T_a, T_{sky}, and T_{gr}, are the ambient, sky, and ground temperature, respectively. Finally, $h_{r,sky}$ and $h_{r,gr}$ are the linearized radiation heat transfer coefficient between the module and the sky and between the module and the ground, respectively. The PV module data sheet provided by the manufacturer shows the effect on the efficiency by the deviation of the solar cell temperature from standard testing conditions (STC).

However, quantifying the effect of irradiance variation on solar cell performance is less straightforward. The overall module efficiency accounting for both temperature and irradiance influence can be approximated as

$$\eta\left(T_M, G_M\right) = \eta\left(25°C, G_M\right)\left[1 + \kappa\left(T_M - 25°C\right)\right] \tag{8}$$

where the first term represents the effect of irradiance and the second that of temperature, with κ computed as:

$$\kappa = \frac{1}{\eta(STC)}\frac{\partial \eta}{\partial T} \tag{9}$$

and representing the temperature effect on the performance relative to the STC conditions efficiency (Smets et al., 2016).

The selected PV module is the 'AstroSemi 365W' mono-crystalline panels from Astronergy. The solar modules have a 365 Wp rated power and a 19.7% efficiency at STC.

2.4. Definition of system performance indicators

The effectiveness of the PV system integration can be assessed by the trolleygrid independence from the AC grid.

PV Utilization, U_{PV}: The PV energy fraction supplying the buses independently of the LVAC (modes 1 and 2 in Fig. 3):

$$U_{PV} \triangleq \frac{\int_{year}(P_{load} - P_{grid})\,dt}{\int_{year} P_{PV}\,dt} \tag{10}$$

with P_{load} the substation demand as seen in Eq. (5), P_{grid} the power delivered by the AC grid, and P_{PV} the PV power.

Direct Load Coverage, Λ: The fraction of the load directly supplied by the PV system:

$$\Lambda \triangleq \frac{\int_{year}(P_{load} - P_{grid})\,dt}{\int_{year} P_{load}\,dt} \tag{11}$$

And finally, the PV system size at a substation can be normalized as the **Energy-Neutrality Ratio**, ζ:

$$\zeta \triangleq \frac{\int_{year} P_{PV}\,dt}{\int_{year} P_{load}\,dt} \tag{12}$$

Ignoring converter losses, the three parameters can be expressed in function of each other by combining Eq. (10), (11), and (12):

$$\Lambda = U_{PV} \cdot \zeta \tag{13}$$

2.5. Case study definition

The trolleygrids of the cities of Arnhem, the Netherlands, and Gdynia, Poland, are taken as case studies for this research. The choice is made for these two cities as they have very different trolleygrid characteristics but a similar solar profile, allowing for a more generalizable study. It is an important validation that despite the stark differences between the trolley networks of Gdynia and Arnhem, the proposed methods in this paper are still valid, as will be shown in the coming sections. Table 1 provides an overview of the key characteristics of the two grids.

Compared to the Arnhem grid, the Gdynia trolleygrid is characterized by double the number of bus lines and bus fleet size and a higher yearly load demand. Meanwhile, the Arnhem grid is fragmented into more sections and substations than the Gdynia grid. Namely, the Arnhem grid is characterized by 43 sections fed by 18 substations, while in Gdynia, 30 sections are fed by 10 substations. Finally, Gdynia substations see about 3 times the average traffic than those in Arnhem would see. These two cities offer thereby two very different trolleygrids infrastructures under a similar sun profile. All PV systems at the substations have been sized for ζ=1 (net energy neutral) unless otherwise stated.

3. Key performance indicators for the U_{PV}

This section presents the Key Performance Indicators (KPIs) that are used in this paper to assess the variation in the PV potential at different substations.

Any variable that influences or measures the direct PV utilization can be traced back to having an effect on, or a measure of any of these three levels:

Table 1
Comparison of the two case study grids of this paper.

Parameter	Gdynia	Arnhem
Number of Bus Lines	12	6
Number of buses	84	42
Number of sections	30	43
Number of SS (Substations)	10	18
Section/Substation ratio	3	2.4
Bus/Substation ratio	8.4	2.3
Average bus traffic per substation	3.1	1.1
Yearly grid energy demand[a] [–]	1.00	0.747
Average yearly SS energy demand [–]	0.10	0.041
Length of sections - average [km]	1.3	1.1
Average daily sunshine duration [h]	4.4	4.0
Average yearly irradiance [kWh/m^2]	225	190

[a]Sensitive information: Normalized to the yearly energy demand of Gdynia.

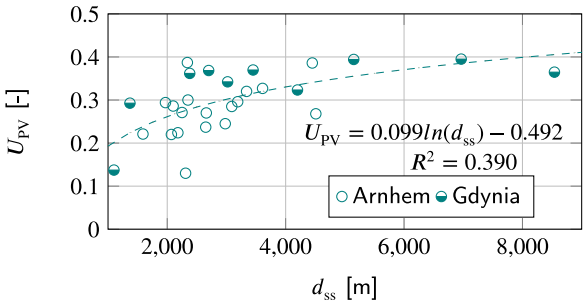

Fig. 5. PV Utilization, U_{PV}, as a function of the distance covered by each substation, d_{ss}. No trend can be concluded for this KPI.

- The **PV Output** (e.g., solar irradiance), and/or
- The **Load** (e.g., HVAC demand), and/or
- The **PV ∩ BUS**, which is the total time duration when there is simultaneously a bus demand (load) and a non-zero PV generation

For example, cloud coverage can affect the **PV Output** by reducing the irradiance, but can also affect the **PV∩BUS** if the clouds would block the sun generation completely. Recurring traffic lights can delay the presence of a bus on a section and cause more regenerative braking, both of which are phenomena that can alter the **Load** under a substation. If the regenerative braking is high enough, the braking bus can completely supply another bus on the section and effectively *mask* it from the PV, affecting the **PV∩BUS**.

Using full-year bus, grid, and PV simulations for all substations in Arnhem and Gdynia, Table 2 summarizes the KPIs studied in this paper, their effect on the three influence levels mentioned above, and their correlations to PV Utilization (curve fit and R-squared values (Wright, 1921)). Five of these KPIs are then explained in detail in the following sections.

3.1. KPI: Yearly irradiance and equivalent sun hours

A sun hour is equivalent to 1000 W/m^2 collected in 1 h of sunlight. Equivalent Sun Hours (ESH) is then not only influenced by the sunrise and sunset times, but also by the local cloudiness that can block out the sun (Wu et al., 2016). This parameter has thereby an impact on the output of the PV installed capacity and on the time of the day during which the trolleybus is able to *see* and utilize this output, i.e., **PV∩BUS**.

In Table 3, the change in U_{PV} and Λ are shown as a function of these two parameters for a median of all studied Gdynia substations. For these simulations, the same PV systems at each substation of Gdynia were subjected to the same bus load demand, yet to different sunshine profile data (read: ESH) of Arnhem, Gdynia, Szeged (Hungary), and Athens (Greece) for one year of operation. The trolleygrid U_{PV} is not affected noticeably between the four cases. On the other hand, the Λ varies by more than 10 percentage points.

This can be better understood when deconstructing the PV Utilization as the result of two mismatches between the traction substation load demand and the PV generation: A temporal or horizontal mismatch (the moments where there is generation but no load, and vice versa), and a power or vertical mismatch (the moments when the generation and load are not equal, but still not zero).

The temporal mismatch (i.e., **PV∩BUS**) can be visualized by revisiting Fig. 2(b), where the effect is clear on the low PV utilization as a consequence of the mismatch between the infrequent bus presence and the PV generation. This is an inherent behaviour in any transportation network. Furthermore, there would be many bus operation hours after sunset (i.e., zero generation), which then adds to this effect.

Secondly, a sunnier city profile means both an increase in sun hours as well as peak irradiance. This means that the increase in ESH is also an increase in the magnitude and frequency of the PV power peaks and its mismatch with the trolleygrid demand, taking away from any obtained U_{PV} advantage from one city sun profile over the other. This means that while sunnier locations offer a better temporal/horizontal match between load and generation, they offset this benefit by a larger power/vertical mismatch, for the same PV system size.

Finally, it might sound counter-intuitive that the same PV system size would have the same utilization when subjected to the much sunnier profile of, for example, a city like Athens. It is good to recall then that the PV Utilization is a parameter that looks at the matching between load and generation, and is normalized to the PV generation (see Eq. (10)). It is the load coverage of Eq. (11) that offers insight into the amount of energy generated. This justifies why, as seen in Table 3, there can be more load coverage (total generation) with a sunny profile while keeping a similar utilization (i.e., *portion* of the power that is not in excess).

In summary, the study of these two sun parameter KPIs in detail justifies the low influence of **PV Output** in Table 2 and the high influence of **PV∩BUS**, on the other hand. This also validates the counter-intuitive phenomena in the later sections of this paper of why both the Arnhem and Gdynia substations, despite their major grid architectural and operational differences, agree on the same KPI trend curves and exhibit a common PV system performance behaviour.

3.2. KPI: Substation total supplied catenary distance: d_{ss}

The increase in the value of this KPI could be expected to reflect higher total demands and traffic under a substation. However, more buses would also mean higher chances of sharing the regenerative braking power, P_{net}, instead of the use of braking resistors, P_{BR}. This could bring down the demand on the substation, P_{load}, creating more excess generation than would have been expected. These opposing phenomena justify the lack of a trend between the U_{PV} and the d_{ss} in Fig. 5. The total length of the supply zone of a substation does not offer a trend as it includes a number of contradicting variables (explained above) and does not offer enough information about the trolleygrid infrastructure and traffic. For example, Substation Q in Arnhem (previously seen in Fig. 2) has a d_{ss} of 2.31k km and a low U_{PV} of 13% as it is covering the low-traffic end-of-line areas of a bus route. On the other hand, Substation D with a similar d_{ss} of 2.34 km and yet a U_{PV} of 38.6% is covering busy and central roads. In short, the d_{ss} parameter carries within it too many contradicting parameters to offer any usable trend for the estimation of PV performance in trolleygrids, and will not be considered any further.

3.3. KPI: Substation yearly energy demand: E_{ss}

The Substation Load Demand gives a direct indication of the bus power demand as well as the bus traffic, and an indirect insight into the bus braking energy recovery. This indirect insight comes from the fact

Table 2
KPIs and their correlation to the PV Utilization, U_{PV}, across all the simulated trolley traction substations of Arnhem (NL) and Gdynia (PL). Both the qualitative assessment of the KPI relationship to the PV output, bus load, or time overlap between buses and PV(H: High, L: Low, **x**: none) and the quantitative assessment of the U_{PV} as a function of the KPI (simulations and best curve-fitting) are presented here.

Substation KPI parameter	Effect on/ Measure of PV Output	Effect on/ Measure of Load	Effect on/ Measure of PV∩BUS	Best fit for $U_{PV}=f$(KPI) [type, R^2]	Comments
Equivalent sun hours, ESH [h]	**H**	x	x	N/A	All substations in a city would have the same value for this KPI; **more details in** Section 3.1
After-sunset fraction of daily bus schedule[%]	**L**	x	**L**	Log, **0.08**	All substations have a value of 10%–20% for this KPI; no correlation can be observed
Yearly average transmission losses [%]	x	**H**	x	Linear, **0.22**	While this KPI gives a clear indication of the bus traffic and load, it offers no insights on the other levels
Total supplied catenary distance, d_{ss} [m]	x	**L**	**L**	Log, **0.39**	Shortcoming: No indication of traffic; e.g: end-of-line sections can be long yet empty; **more details in**Section 3.2
Specific Traffic KPI $\overline{N_{bus}}/d_{ss}$ [bus/km]	x	**L**	**L**	Log, 0.51	Shortcoming: Same KPI value if 2bus/1km or 1bus/0.5km, overlooking their different braking energy recovery & PV∩BUS
Specific Energy KPI E_{ss}/d_{ss} [MWh/km]	x	**H**	**L**	Log, 0.63	Shortcoming: Despite high bus and traffic insight, not much indication into the section length and hence not into PV∩BUS
Yearly average bus traffic: $\overline{N_{bus}}$ [bus]	x	**H**	**L**	Log, 0.84	Shortcoming: Similar substation KPI value if 1 bus, or if 2 buses half the time and 0 otherwise; **more details in**Section 3.4
Distance energy KPI $E_{ss} \cdot d_{ss}$ [MWh.km]	x	**L**	**H**	Log, 0.86	Shortcoming: Similar KPI values for long sections with low energy demand and short sections with high demand
Traffic distance KPI $\overline{N_{bus}} \cdot d_{ss}$ [bus.km]	x	**L**	**H**	Log, 0.86	Shortcoming: Similar KPI values for long sections of low traffic and short sections of high traffic
Yearly energy demand: E_{ss} [MWh]	x	**H**	**H**	Log, **0.93**	**More details in**Section 3.3
Traffic energy KPI: $E_{ss} \cdot \overline{N_{bus}}$ [MWh.bus]	x	**H**	**H**	Log, **0.91**	**More details in** Section 3.5

Table 3
Change of the U_{PV} and Λ (in percentage points) for the same PV system (sized for Gdynia as a benchmark) when subjected to the yearly sun profiles of different cities.

Sun profile	Gdynia	Arnhem	Szeged	Athens
ESH [h]	4.4	4.0	5.5	7.6
Irradiance [W/m^2]	140	130	180	210
PV System Total Size (at all substations) [MWp]	6.57 (ζ=1)	Gdynia system	Gdynia system	Gdynia system
Change in Grid Median U_{PV} [percentage points]	benchmark	+1.4	−0.9	−1.3
Change in Grid Median Λ [percentage points]	benchmark	−0.5	+5.5	+10

that high utilization of braking energy would already be reflected in a lower substation demand. These powerful insights can be contrasted with the d_{ss} KPI which would not offer information on the traffic and braking.

Fig. 6 shows the correlation between the PV utilization and the substation energy demand in MWh. A strong logarithmic correlation exists with an R^2 value of over 0.93, indicating a good fit.

This fit seems to reach a plateau (the red dotted line) for values over 600 MWh. The substations of 686 and 1298 MWh report almost the same PV utilization at 36.18% and 36.97%, respectively. The 5 substations in between, a mix of Arnhem and Gdynia substations, hover around this same U_{PV} value.

This contradicts the previous proposition in the literature that a larger substation would always see a better PV utilization

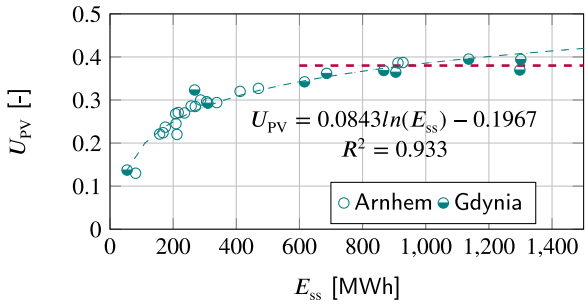

Fig. 6. PV Utilization, U_{PV}, as a function of energy demand of each substation, E_{ss}. A plateau is observable starting 600 MWh.

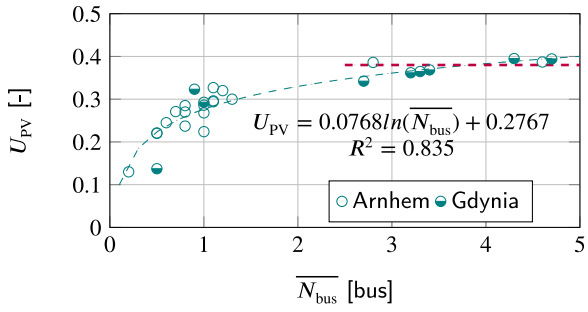

Fig. 7. PV Utilization, U_{PV}, as a function of the substation average traffic, $\overline{N_{bus}}$. A plateau is observable starting 2.5bus.

(Bartłomiejczyk, 2018b; Wazifehdust et al., 2019; Diab et al., 2022e). The main reason is that PV utilization is also subject to seasonal variations. The large PV systems would over-produce in the high-irradiance summer months when the buses typically run on less-frequent timetables and without the considerable HVAC heating demand. Large PV systems, therefore, would see a low utilization in the summer months, bringing down their average yearly U_{PV} value.

3.4. KPI: Substation yearly average bus traffic: $\overline{N_{bus}}$

Another important, and yet readily available grid parameter is the average traffic under a substation, $\overline{N_{bus}}$, from bus schedules. A trend is also observable in Fig. 7, although its R^2 value is only at 0.835, which is lower than the one found between U_{PV} and E_{ss}. However, the advantage of this KPI is that it visually disperses the substations on the trend curve more than the previous KPI. For example, the two Arnhem substations of around 900MWh are now considerably apart, at values of $\overline{N_{bus}}$ equal to 2.8 and 4.6. However, the two substations share the same U_{PV} (38.6% and 38.7%). This confirms the existence of a plateau in the PV Utilization and motivates the inclusion of $\overline{N_{bus}}$ in the performance estimation. The U_{PV} plateau can be observed in Fig. 7 for values of $\overline{N_{bus}}$ above 2.5 bus (red dotted line).

These plateaus are an unavoidable consequence of both the daily mismatch between the intermittent bus scheduling and the PV generation (recall Fig. 2), and the seasonal mismatch explained in the previous KPI subsection. This urges trolleygrid cities to integrate more smart grid components such as electric vehicle chargers or stationary storage systems into their infrastructure in the hope of increasing the substation U_{PV} values. These additional base loads can thereby help push this intrinsic saturation plateau to higher performance values by utilizing the PV generation when there is no (or little) bus demand, making the PV system more economically feasible and reducing the need for storage, exchange with the AC grid, or curtailment.

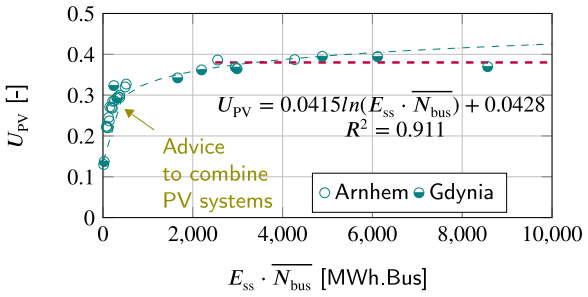

Fig. 8. PV Utilization, U_{PV}, as a function of the substation traffic energy, $E_{ss} \cdot \overline{N_{bus}}$. A plateau is observable starting at 2200 MWh.Bus and underachieving substations (left-hand group) are exposed.

3.5. KPI: Substation traffic energy: $E_{ss} \cdot \overline{N_{bus}}$

To combine the trend of the energy substation demand KPI, E_{ss}, and the dispersing effect of the substation average bus traffic KPI, $\overline{N_{bus}}$, a new KPI is defined as the substation Traffic Energy: $E_{ss} \cdot \overline{N_{bus}}$.

Although this KPI does not have a physical interpretation, it mathematically combines two important trolleygrid substations parameters and offers insights into PV utilization and sizing. In Fig. 8, the substations clearly communicate whether they are at the plateau of performance, or whether they are *behind the knee* of the performance curve. This offers a clear insight to trolleygrid operators on which PV systems need to be resized and/or combined with other systems. Section 5 addresses this latter topic in more detail.

Another advantage of this KPI over the E_{ss} KPI is that it better estimates the performance of a combined PV system (a PV system serving multiple substations). For example, a centralized PV system for the whole Arnhem grid has a U_{PV} of 42% from previous simulations by the authors of this paper in Diab et al. (2022e). The E_{ss} KPI curve would over-estimate this at 53%, while the Energy Traffic KPI curve places it at 41%. Section 5 addresses the topic of substation combination in more detail.

4. U_{PV} performance estimation

The strong trend between U_{PV} and $E_{ss} \cdot \overline{N_{bus}}$ observed in Fig. 8 for energy-neutral PV system sizes (ζ=1) can also be observed for other system sizes, as reported in Fig. 9. These trends at different system sizes observed are of the form $a \cdot ln(E_{ss} \cdot \overline{N_{bus}}) + b$. The a and b coefficients of the different curves are plotted in Fig. 10 as a function of the normalized system size (ζ of Eq. (12)), and described analytically in Eq. (14) and (15). This method, summarized by the flowchart of Fig. 11, offers then a quick and straightforward way for the U_{PV} estimation of any PV system at any substation without the need for complex grid and PV models.

$$a = 0.0215\zeta^3 - 0.1494\zeta^2 + 0.3369\zeta - 0.1680, \quad R^2 = 0.998 \tag{14}$$

$$b = -0.0082\zeta^3 + 0.0553\zeta^2 - 0.1305\zeta + 0.1244, R^2 = 1 \tag{15}$$

5. Suggested sizing approach for substation combination

The logarithmic trends described in this paper showed a sharp rise in PV system performance, followed by a saturation plateau. Any substation sitting before the knee-point on the performance curve is then experiencing a lower U_{PV} than is achievable for other substations in their city with a higher Traffic Energy KPI.

This invites the installation of a semi-decentralized PV system combining service to neighbouring substations in a way that moves their combined performance towards the knee and the plateau of the utilization curve. An example of these substations is highlighted in Fig. 8 (golden arrow).

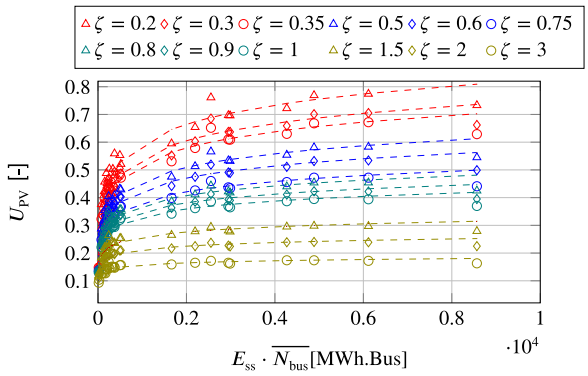

Fig. 9. PV Utilization, U_{PV}, of Arnhem and Gdynia substations for different PV system sizes (as the energy-neutrality ratio ζ) against the defined Traffic Energy KPI $E_{ss} \cdot \overline{N_{bus}}$[MWh.Bus]. This is an extension of Fig. 8 for any ζ between 0.2 and 3.

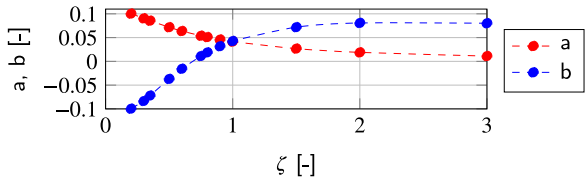

Fig. 10. Coefficients a and b for the different ζ of Fig. 9.

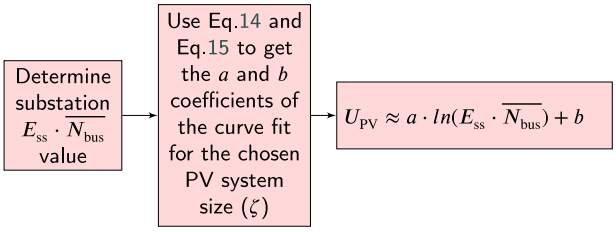

Fig. 11. The proposed methodology in this paper to approximate the PV utilization of a trolleybus substation using the suggested, empirically-derived third-degree polynomial and without the need for complex PV, bus, or grid modelling.

On the other hand, substations already on the plateau should not be destined for large PV system sizes as their utilization saturates rapidly. In fact, they should be sized at a value lower than energy-neutral sizes (i.e. ζ <1) as they can offer high U_{PV} values at these small system sizes (Fig. 9), and bring thereby a better technical and economical feasibility. Obviously, at those sizes, however, the load coverage will not be high as can be predicted by Eq. (13). This bespoke trade-off is left to the stakeholders.

Cities aiming to build new, sustainable trolleygrids should also be aware of the saturation points in the curve because larger, higher traffic substations would come with higher transmission losses, for the same fraction of U_{PV}, as the resulting large system size would probably need to be built at a distance from the substations, with additional transmission cables.

Fig. 12 shows the example of combining two or three neighbouring Arnhem substations of low U_{PV}. Two important observations can be reported. Firstly, the combined PV system does indeed outperform any of its individual constituents, validating this encouraging message to trolleygrid cities to adopt this sizing method. This is a consequence of the higher traffic and continuous load that a combination of substations can offer, compared to a single substation. This brings about a better match between the PV generation and the substation load. Mathematically, this translated to a higher Traffic Energy KPI value. Secondly, a greatly beneficial result is that the performance of the combined PV systems can also be estimated using the previously reported trends as

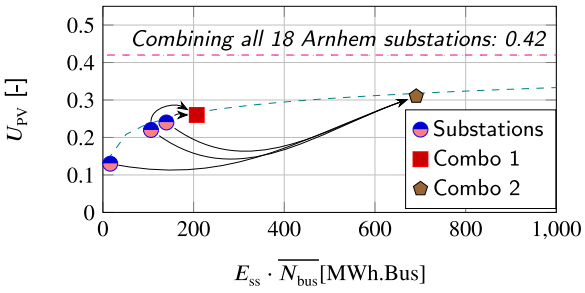

Fig. 12. Example of the suggested sizing method: The U_{PV} of three neighbouring Arnhem PV systems and of two of their combinations. As expected, the combinations outperform their individual constituents and their U_{PV} also sits on the same prediction trend curve derived in this paper.

these combos also sit on the trend curve. As explained in the previous section, this KPI curve can also be used up to the whole city grid (centralized PV system) as verified by comparing the results to those from the previous calculations in Diab et al. (2022e).

6. Conclusions

PV integration in urban transportation networks so far neither has a clear methodology or consensus for the placement and sizing of PV systems, nor an available tool to easily estimate the performance of the PV systems. This paper offered a simple approach for PV integration in trolleybus grids by examining two case study cities of very different characteristics of trolleygrid architecture, bus traffic, and substation power demands. However, common trends for both cities were still observed. A number of KPIs were studied, but a strong trend was reported between the PV direct utilization and the here-defined KPI of Substation Traffic Energy - a multiplication of the yearly energy demand of the substation and the average traffic it sees. This empirically derived, logarithmic trend of the form $a \cdot ln(E_{ss} \cdot \overline{N_{bus}}) + b$ was also shown to be extendable to different PV system sizes, and the a and b coefficients were analytically described using a simple third-degree polynomial for any normalized PV system size ζ. This allows now trolleybus cities to quickly and efficiently estimate the performance of any PV system on any substation without the need for the complex grid, PV, and bus modelling. Moreover, the trends observed offer strong insights and advice to these cities on where the placement and sizing of the PV systems and how to combine substations for increased benefit.

The paper also exposed performance saturation plateaus not previously reported in the literature. These plateaus are an uncompromising consequence of the mismatch between the intermittent bus scheduling and the PV generation that is to be expected in any trolley city that does not integrate more smart grid loads into its trolleygrid infrastructure.

Future work is urged on the integration of more base loads (such as electric vehicle chargers) in trolleygrids to push this plateau to higher performance values. Additionally, storage systems should be studied for the same motive. Finally, despite the fact that the first KPI (Yearly Irradiance and Sunshine Duration) showed a weak trend between the PV input parameters and the PV utilization, more work is invited on including more cities of different sunshine profiles to further confirm that the offered polynomial fit is indeed suitable for the study of different trolleygrid cities.

CRediT authorship contribution statement

Ibrahim Diab: Conceptualization, Methodology, Software, Validation, Investigation, Data curation, Writing – original draft. **Alice Saffirio:** Software, Validation, Investigation, Data curation, Writing – review & editing. **Gautham Ram Chandra-Mouli:** Funding acquisition, Project administration, Supervision, Writing – review & editing, Resources. **Pavol Bauer:** Funding acquisition, Project administration, Supervision, Writing – review & editing, Resources.

Declaration of competing interest

The authors declare that they have no known competing financial interests or personal relationships that could have appeared to influence the work reported in this paper.

Data availability

Data will be made available on request.

References

Arboleya, P., Mohamed, B., El-Sayed, I., 2018. DC railway simulation including controllable power electronic and energy storage devices. IEEE Trans. Power Syst. 33 (5), 5319–5329.

Barbone, R., Mandrioli, R., Ricco, M., Paternost, R.F., Cirimele, V., Grandi, G., 2022. Novel multi-vehicle motion-based model of trolleybus grids towards smarter urban mobility. Electronics 11 (6), 915.

Bartłomiejczyk, M., 2018a. Dynamic Charging of Electric Buses. Gdańsk University of Technoligy, Faculty of Electrical and Control Engineering, URL https://books.google.cz/books?id=ziX_vQEACAAJ.

Bartłomiejczyk, M., 2018b. Potential application of solar energy systems for electrified urban transportation systems. Energies 11 (4), 954.

Bartłomiejczyk, M., Hołyszko, P., Filipek, P., 2016. Measurement and analysis of transmission losses in the supply system of electrified transport. J. Ecol. Eng. 17 (5).

Bartłomiejczyk, M., Kołacz, R., 2020. The reduction of auxiliaries power demand: The challenge for electromobility in public transportation. J. Clean. Prod. 252, 119776.

Bartłomiejczyk, M., Połom, M., 2015. Spatial aspects of tram and trolleybus supply system. In: 8th International Scientific Symposium on Electrical Power Engineering. ELEKTROENERGETIKA, pp. 223–227.

Bartłomiejczyk, M., Połom, M., 2015b. Spatial aspects of tram and trolleybus supply system. In: 8th International Scientific Symposium on Electrical Power Engineering. ELEKTROENERGETIKA, pp. 223–227.

Bartłomiejczyk, M., Połom, M., 2017. The impact of the overhead line's power supply system spatial differentiation on the energy consumption of trolleybus transport: Planning and economic aspects. Transport 32 (1), 1–12.

Brinkel, N., Gerritsma, M., AlSkaif, T., Lampropoulos, I., van Voorden, A., Fidder, H., van Sark, W., 2020. Impact of rapid PV fluctuations on power quality in the low-voltage grid and mitigation strategies using electric vehicles. Int. J. Electr. Power Syst. Energy 118, 105741.

Chymera, M.Z., Renfrew, A.C., Barnes, M., Holden, J., 2010. Modeling electrified transit systems. IEEE Trans. Veh. Technol. 59 (6), 2748–2756.

Diab, I., Chandra Mouli, G.R., Bauer, P., 2022a. A review of the key technical and non-technical challenges for sustainable transportation electrification: A case for urban catenary buses. In: Proceedings of the 20th IEEE International Power Electronics and Motion Control Conference. IEEE-PEMC 2022, IEEE, pp. 439–448.

Diab, I., Mouli, G.R.C., Bauer, P., 2022b. Increasing the integration potential of EV chargers in DC trolleygrids: A bilateral substation-voltage tuning approach. In: 2022 International Symposium on Power Electronics, Electrical Drives, Automation and Motion. SPEEDAM, pp. 264–269. http://dx.doi.org/10.1109/SPEEDAM53979.2022.9841989.

Diab, I., Mouli, G.R.C., Bauer, P., 2022c. Toward a better estimation of the charging corridor length of in-motion-charging trolleybuses. In: 2022 IEEE Transportation Electrification Conference & Expo. ITEC, pp. 557–562. http://dx.doi.org/10.1109/ITEC53557.2022.9814021.

Diab, I., Saffirio, A., Chandra Mouli, G.R., Singh Tomar, A., Bauer, P., 2022d. A complete DC trolleybus grid model with bilateral connections, feeder cables, and bus auxiliaries. IEEE Trans. Intell. Transp. Syst. 1–12. http://dx.doi.org/10.1109/TITS.2022.3157080.

Diab, I., Scheurwater, B., Saffirio, A., Chandra-Mouli, G.R., Bauer, P., 2022e. Placement and sizing of solar PV and wind systems in trolleybus grids. J. Clean. Prod. 352, 131533.

Finlayson, A., Goodman, C., White, R., 2006. Investigation into the computational techniques of power system modelling for a DC railway.

Hamacek, Š., Bartłomiejczyk, M., Hrbáč, R., Mišák, S., Stýskala, V., 2014. Energy recovery effectiveness in trolleybus transport. Electr. Power Syst. Res. 112, 1–11.

Iannuzzi, D., Lauria, D., Tricoli, P., 2012. Optimal design of stationary supercapacitors storage devices for light electrical transportation systems. Opt. Eng. 13 (4), 689–704.

IEA, 2020. Data overview, electricity statistics, vol. 2021, no. 05/02. URL https://www.iea.org/subscribe-to-data-services/electricity-statistics.

KNMI, 2019. Meteorological data downloaded with meteonorm.

Kratz, S., Krueger, B., Wegener, R., Soter, S., 2018. Integration of photovoltaics into a smart trolley system based on SiC-technology. In: 2018 IEEE 7th International Conference on Power and Energy. PECon, IEEE, pp. 168–173.

Kratz, S., Schmidt, A., Krueger, B., Wegener, R., Soter, S., 2019. Power supply of a short-range public transportation system based on photovoltaics-potential analysis and implementation. In: 2019 IEEE 46th Photovoltaic Specialists Conference. PVSC, IEEE, pp. 3077–3081.

Ku, B.-Y., Liu, J.-S., 2002. Solution of DC power flow for nongrounded traction systems using chain-rule reduction of ladder circuit Jacobian matrices. In: ASME/IEEE Joint Railroad Conference. IEEE, pp. 123–130.

Liu, Y., Chen, M., Cheng, Z., Chen, Y., Li, Q., 2021. Robust energy management of high-speed railway co-phase traction substation with uncertain PV generation and traction load. IEEE Trans. Intell. Transp. Syst..

Paternost, R.F., Mandrioli, R., Barbone, R., Cirimele, V., Loncarski, J., Ricco, M., 2022. Impact of a stationary energy storage system in a DC trolleybus network. In: 2022 IEEE Transportation Electrification Conference & Expo. ITEC, IEEE, pp. 1211–1216.

Salih, M., Baumeister, D., Wazifehdust, M., Steinbusch, P., Zdrallek, M., Mour, S., Deskovic, P., Küll, T., Troullier, C., 2018. Optimized Positioning for Storage Systems in an LVDC Traction Grid with Non-Receptive Power Sources and Photovoltaic Systems. Chair of Power System Engineering University of Wuppertal (October 2019).

Salih, M., Koch, M., Baumeister, D., Wazifehdust, M., Steinbusch, P., Zdrallek, M., 2019. Adapted Newton-Raphson power flow method for a DC traction network including non-receptive power sources and photovoltaic systems. In: 2019 IEEE PES Innovative Smart Grid Technologies Europe. ISGT-Europe, IEEE, pp. 1–5.

Sindi, E., Polis, M., Yin, G., Ding, L., et al., 2018. Distributed optimal power and voltage management in dc microgrids: Applications to dual-source trolleybus systems. IEEE Trans. Transp. Electrif. 4 (3), 778–788.

Smets, A.H., Jäger, K., Isabella, O., van Swaaij, R., Zeman, M., 2016. Solar Energy: The physics and engineering of photovoltaic conversion technologies and systems. UIT.

Tomar, A.S., Veenhuizen, B., Buning, L., Pyman, B., 2018. Estimation of the size of the battery for hybrid electric trolley busses using backward quasi-static modelling. In: Multidisciplinary Digital Publishing Institute Proceedings, Vol. 2, no. 23. p. 1499.

Wang, C., Cai, W., Lu, X., Chen, J., 2007. CO2 mitigation scenarios in China's road transport sector. Energy Convers. Manage. 48 (7), 2110–2118.

Warin, Y., Lanselle, R., Thiounn, M., 2011. Active substation. In: World Congress on Railway Research. Lille, pp. 22–26.

Wazifehdust, M., Baumeister, D., Salih, M., Steinbusch, P., Zdrallek, M., Mour, S., Troullier, C., 2019. Potential analysis for the integration of renewables and EV charging stations within a novel LVDC smart-trolleybus grid. (ISSN: 2960241509).

Wright, S., 1921. Correlation and causation.

Wu, B., Liu, S., Zhu, W., Yu, M., Yan, N., Xing, Q., 2016. A method to estimate sunshine duration using cloud classification data from a geostationary meteorological satellite (FY-2D) over the Heihe river basin. Sensors 16 (11), 1859.

Zahedmanesh, A., Muttaqi, K.M., Sutanto, D., 2021. A cooperative energy management in a virtual energy hub of an electric transportation system powered by PV generation and energy storage. IEEE Trans. Transp. Electrif..

Zhang, D., Jiang, J., Zhang, W., et al., 2015. Robust and scalable management of power networks in dual-source trolleybus systems: A consensus control framework. IEEE Trans. Intell. Transp. Syst. 17 (4), 1029–1038.

Zhang, D., Jiang, J., Zhang, W., et al., 2017. Optimal power management in DC microgrids with applications to dual-source trolleybus systems. IEEE Trans. Intell. Transp. Syst. 19 (4), 1188–1197.

Zhu, X., Hu, H., Tao, H., He, Z., 2019. Stability analysis of PV plant-tied MVDC railway electrification system. IEEE Trans. Transp. Electrif. 5 (1), 311–323.